Article

Daytime radiative cooling using near-black infrared emitters

Jun-long Kou, Zoila Jurado, Zhen Chen, Shanhui Fan, and Austin J. Minnich

ACS Photonics, **Just Accepted Manuscript** • DOI: 10.1021/acsphotonics.6b00991 • Publication Date (Web): 03 Feb 2017

ACS Photonics is published by the American Chemical Society. 1155 Sixteenth Street N.W., Washington, DC 20036

Daytime radiative cooling using near-black infrared emitters

Jun-long Kou, † Zoila Jurado, † Zhen Chen, ‡ Shanhui Fan, ‡ and Austin J. Minnich *,†

†*Division of Engineering and Applied Science, California Institute of Technology, Pasadena, California 91125, USA.*

‡*Ginzton Laboratory, Department of Electrical Engineering, Stanford University, Stanford, California 94305, USA.*

E-mail: aminnich@caltech.edu

Abstract

Recent works have demonstrated that daytime radiative cooling under direct sunlight can be achieved using multilayer thin films designed to emit in the infrared atmospheric transparency window while reflecting visible light. Here, we demonstrate that a polymer-coated fused silica mirror, as a near-ideal blackbody in the mid-infrared and near-ideal reflector in the solar spectrum, achieves radiative cooling below ambient air temperature under direct sunlight (8.2 °C) and at night (8.4 °C). Its performance exceeds that of a multilayer thin film stack fabricated using vacuum deposition methods by nearly 3 °C. Furthermore, we estimate the cooler has an average net cooling power of about 127 Wm^{-2} during daytime at ambient temperature even considering the significant influence of external conduction and convection, more than twice that reported previously. Our work demonstrates that abundant materials and straight-forward fabrication can be used to achieve daytime radiative cooling, advancing applications such as dry cooling of thermal power plants.

Keywords

passive radiative cooling, thermal radiation, infrared emitters

Manipulating thermal emission from surfaces by thermal photonic design has received great attention in recent years.[1–11] In particular, passive radiative cooling schemes that do not require external active devices such as fans, air conditioners or thermoelectrics are of much interest because of their potential to reduce energy consumption.[12–16] Radiative cooling refers to the physical process by which a body dissipates heat to another body of lower temperature via thermal radiation. The coldest known heat sink is the universe with a temperature of around 3 K, and radiative thermal contact can be made with this thermal reservoir by exchanging energy through the transparency window of the atmosphere. Historically, radiative cooling during nighttime has been widely studied and employed for rooftop cooling.[14,17–20] However, radiative cooling during daytime is more useful as cooling demand peaks during daytime hours.

Recently, a passive radiative cooling scheme has been reported by Raman et al. that achieves this goal by radiating energy through the main atmospheric transparency window in the range of 8 - 13 μm while reflecting incident sunlight.[6] Their radiative cooler consisted of seven alternating layers of SiO_2 and HfO_2 on top of a silver back reflector, resulting in 97% reflection of solar illumination and an average emissivity of about 0.65 in the transparency window. With a relatively simple experimental apparatus, Raman et al. was able to achieve a 5 °C degree reduction below the ambient air temperature under direct sunlight. Subsequently, Chen et al. was able to demonstrate an average temperature reduction of 37 °C below ambient by combining a selective emitter with an apparatus consisting of a vacuum chamber.[21] Related to these experiments, there have been other recent theoretical works in designing various photonic structures for radiative cooling purposes.[12,22–25]

Most of these radiative coolers are designed to emit only in the atmospheric transparency window to avoid exchanging radiation with the atmosphere. This requirement leads to complex photonic designs, for instance consisting of multilayer stacks that require vacuum deposition methods. It is interesting to consider whether emitting and absorbing outside of the main atmospheric transparency window is necessarily detrimental. If not, materials that are naturally visibly transparent yet emit strongly over a broad bandwidth in the mid-infrared, such as glasses, could perform as well as other more complex photonic structures reported previously.

Here, we experimentally demonstrate passive radiative cooling under direct sunlight and at night using only a polymer-silica-mirror consisting of a fused silica wafer coated with a polymer top layer and a silver back reflector. This simple scheme achieves daytime cooling temperature differentials of 8.2 °C under direct sunlight and 8.4 °C at night, nearly 3 °C larger than that achieved by the nanophotonic structure in daytime. Our work demonstrates that inexpensive, abundant materials can be used for applications in energy such as dry cooling for power plants by realizing daytime radiative cooling without need for complex photonic structures.

We experimentally examine the radiative cooling performance of the polymer-silica-mirror by coating a 4-inch fused silica wafer of 500 μm thickness with a 100 μm thick polydimethylsiloxane (PDMS) film as a top layer and 120 nm thick silver film as a back reflector. The silver film is deposited by electron beam evaporation method under high vacuum. The PDMS film is spin-coated for 60 seconds followed by degassing for 10 minutes and curing for one hour at 80 °C. The performance of the device is tested on the roof of a building in Pasadena, California by exposing it to the sky.

A picture of the setup and surroundings is shown in Figure 1a. To experimentally achieve cooling below ambient, special care needs to be taken in the measurement setup to reduce the parasitic conduction and convection from the ambient. In our measurement, the device is placed on a low thermal conductivity aerogel blanket which is attached to the inner side of a petri-dish. The petri-dish is supported by three glass rods to suspend it above the roof. The top of the petri-dish is covered by a polyethylene film, acting as a convection shield that is transparent to all the radiative wavelengths of interest. The temperatures of the device and ambient air are recorded by K-type thermocouples.

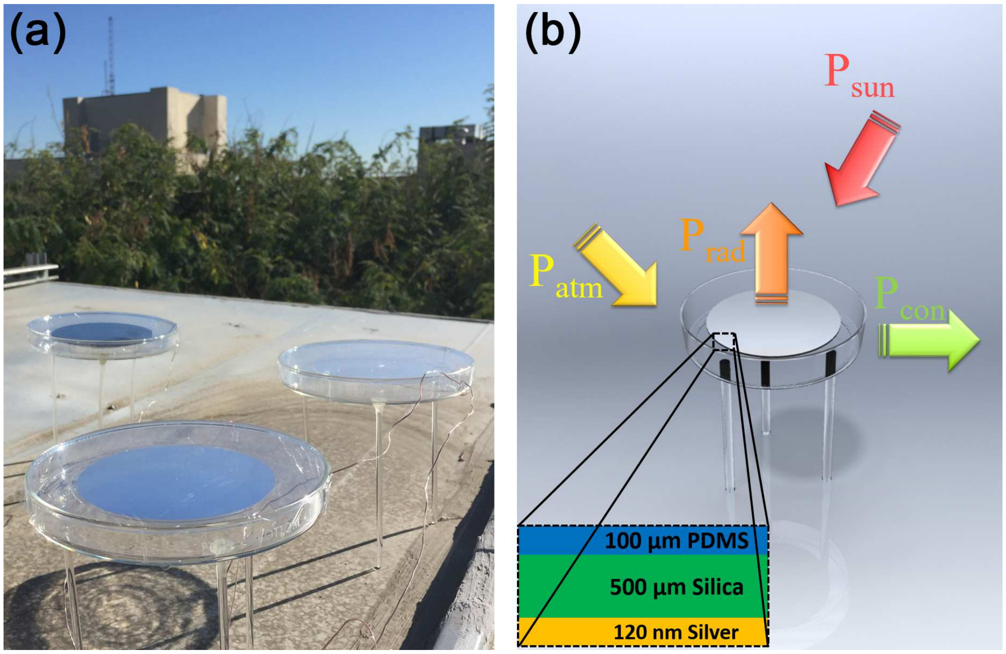

Figure 1: (a) Image of the samples under field test on the roof of a building in Pasadena, California. The device sits on top of an aerogel blankets attached to the bottom surface of a petri-dish with full access to the sky. The petri-dish is supported by three glass rods, suspending the petri-dish from the roof. The top of the petri-dish is covered by polyethylene film, acting as a convection shield that is transparent to all the radiative wavelengths of interest. (b) Schematic of the test setup. The input/output energy balance is labeled with P_{rad}, P_{sun}, P_{atm} and P_{con} denoting the radiated power from the cooler, absorbed power from the sun, absorbed power from the atmosphere, and conduction/convection power loss, respectively. The inset in (b) shows the cross section of the cooler structure consisting three layers.

The measured temperatures of the polymer-silica-mirror, silica-mirror without polymer coating and the ambient air are shown in Figure 2. The polymer-silica-mirror maintains a temperature that on average is 8.2 °C below the ambient air temperature throughout the period when it is exposed to the sun. At night, the device achieves 8.4 °C below ambient air temperature without sun irradiation. The daytime temperature differential is 1.0 °C larger than the silica-mirror and nearly 3 °C larger than that of a prior report.[6] For comparison, we also include the field test results of a doped silicon wafer (resistivity of 8 - 12 Ω-cm) measured under the same conditions. Its temperature increases significantly after exposure to sunlight, reaching nearly 57 °C under the peak solar irradiation. Interestingly, the doped silicon wafer also exhibits radiative cooling of about 5 °C below ambient air temperature after sunset, indicating the cooling ability of silicon solar cells. Here, the infrared absorption and emission is due to free carriers introduced by the doping.

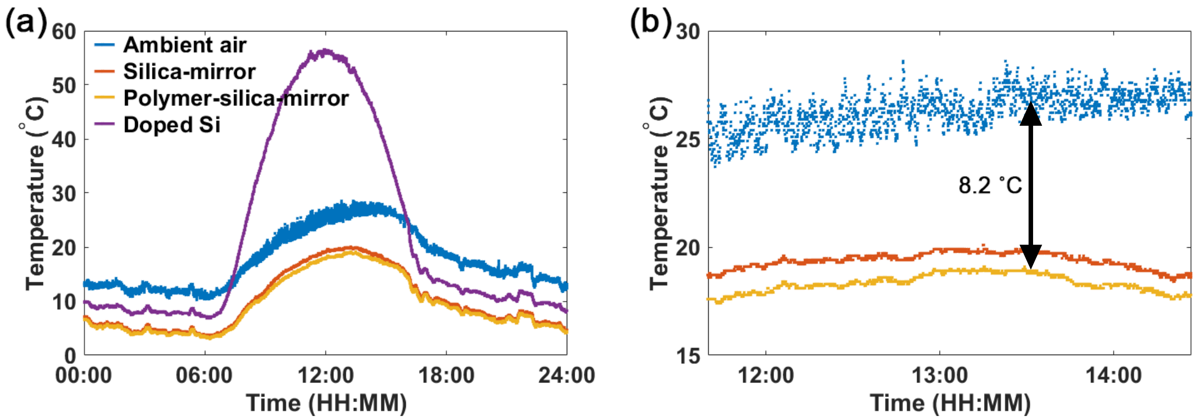

Figure 2: (a) Temperature measurement of the polymer-silica-mirror (orange), silica-mirror (red), ambient air temperature (blue) and bare doped silicon wafer (purple) during a 24-hour cycle. (b) Zoom-in of the temperature measurement when the device is under direct solar irradiation. The polymer-silica-mirror achieves a temperature that is 8.2 °C below ambient air temperature under these conditions.

To understand these observations, we measure the emissivity of the samples over the visible and infrared wavelength ranges using an ultraviolet/visible/near-infrared spectrometer and Fourier transform infrared spectroscopy (FTIR). The result is shown in Figure 3. Due to the transparency of fused silica and PDMS as well as the high reflectivity of silver from the visible to the near-infrared, the absorption for these wavelengths is minimal. However, a significant portion of the ultraviolet light is absorbed by the samples, resulting in about 23 Wm^{-2} absorption power density for the polymer-silica-mirror. The emissivity approaches unity for infrared wavelengths longer than 4.5 microns due to absorption of PDMS and silica. Here, PDMS is added to the design to counteract the large absorption dip of fused silica around wavelengths of 9 microns, shown as the red line in Figure 3. Counterintuitively, despite the fact that the sample has a high absorption outside the main atmospheric transparency window, we observe radiative cooling performance exceeding that of the nanophotonic cooler designed to emit only within the atmospheric transparency window of Raman et al.[6]

We investigate the origin of this observation by calculating the cooling performance of two additional cases with idealized emissivity profiles shown in Figure 3. For Case 1, the emissivity is unity beyond 4.5 μm and zero otherwise, while for Case 2 the emissivity is only unity in the main atmospheric transparency window.

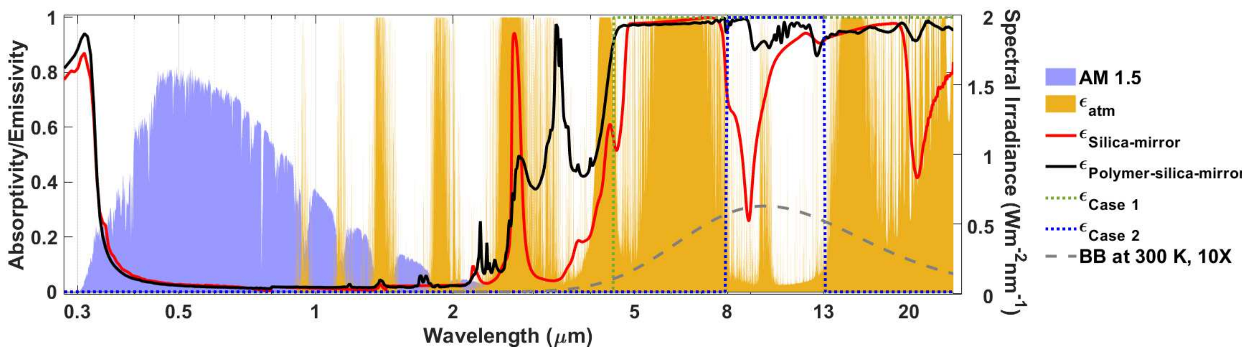

Figure 3: Measured emissivity of the polymer-silica-mirror (black solid line) and silica-mirror (red solid line) from ultraviolet to far infrared. Emissivity of two idealized cases: Case 1 (green dashed line) with unity emissivity beyond 4.5 μm and Case 2 (blue dashed line) with unity emissivity only in the main atmospheric transparency window. The AM 1.5 solar spectrum, atmospheric absorption spectrum and a blackbody radiation curve (grey dashed line, 10 times enlarged in spectral irradiance) at 300 K are superimposed.

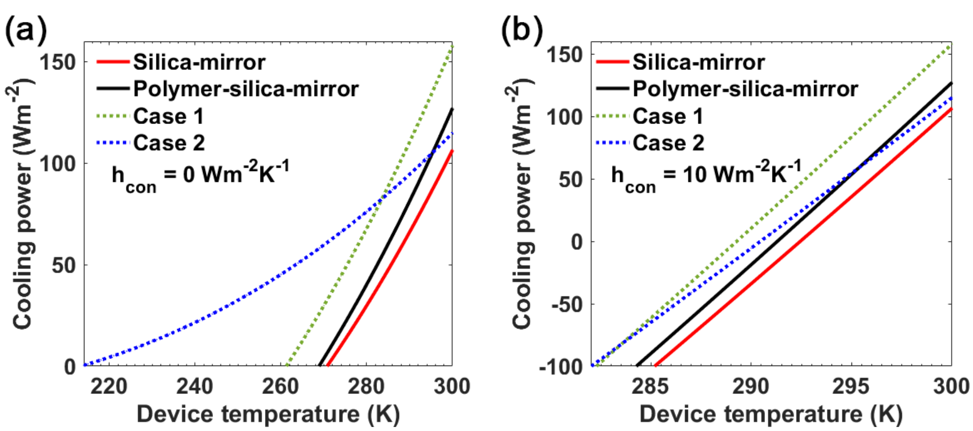

Figure 4: Calculated net cooling power density of the polymer-silica-mirror, silica-mirror and the two idealized cases as a function of device temperature with different thermal coefficients (a) $h_{con} = 0$ and (b) $h_{con} = 10$ Wm^{-2}K^{-1} under AM 1.5 illumination. The ambient temperature of the atmosphere is taken to be 300 K.

We begin by examining the radiative energy balance of the coolers under solar illumination. We take the cooler to be at temperature T_{dev} and the ambient atmospheric temperature to be T_{amb}. The net cooling power density, defined as P_{cool}, is given by:

$$P_{cool} = P_{rad}(T_{dev}) - P_{sun} - P_{atm}(T_{amb}) - P_{con}(T_{amb}, T_{dev}) \tag{1}$$

where P_{rad} denotes the radiation power density of the device:

$$P_{rad}(T_{dev}) = \int d\Omega \cos(\theta) \int d\lambda I_{BB}(T_{dev}, \lambda)\epsilon_{dev}(\lambda, \theta) \tag{2}$$

with I_{BB} indicating the spectral radiance of a blackbody, ϵ_{dev} being the emissivity of the cooler and λ being the wavelength. The absorbed power density by the device with surface facing the sun at angle Ψ is given by:

$$P_{sun} = \cos(\Psi) \int d\lambda \epsilon_{dev}(\lambda, \Psi) I_{AM1.5}(\lambda) \tag{3}$$

$I_{AM1.5}$ is used as solar illumination intensity during daytime and Ψ is the angle between the normal direction of the cooler and the sun. The absorbed power density due to surrounding atmospheric thermal radiation is:

$$P_{atm}(T_{amb}) = \int d\Omega \cos(\theta) \int d\lambda I_{BB}(T_{amb}, \lambda)\epsilon_{dev}(\lambda, \theta)\epsilon_{atm}(\lambda, \theta) \tag{4}$$

The emissivity of the atmosphere is given by $\epsilon_{atm}(\lambda, \theta)$.[26] The last term from Equation (1) is the power density of thermal conduction and convection parasitically transferred to the cooler:

$$P_{con}(T_{amb}, T_{dev}) = h_{con}(T_{amb} - T_{dev}) \tag{5}$$

where h_{con} is the thermal coefficient. Experimentally, the thermal coefficient is determined by heating up a 4-inch Si wafer and measuring the transient temperature of the wafer in the same petri-dish used for the radiative cooler. For this measurement, we maximize the influence of parasitic conduction and convection by coating the wafer with silver on both polished sides, thereby minimizing radiative losses. Fitting the transient temperature using a lumped capacitance analysis yields the thermal coefficient as around 10 $Wm^{-2}K^{-1}$.

We present the net cooling power density as a function of device temperature without and with the influence of parasitic convection and conduction in Figures 4a and b, respectively. The figure shows that Case 1, which emits outside the primary atmospheric transparency window and thus parasitically absorbs radiation from the atmosphere, has a larger cooling power density than Case 2 for cooler temperatures above 283 K. While the absorbed atmospheric radiation increases for Case 1, the power radiated outward increases by a larger amount. Thus, expanding the spectral range of high emissivity can be beneficial under some circumstances.[21,25] For a cooler temperature of 300 K, Case 1 achieves a cooling power density 158 Wm^{-2}, 43 Wm^{-2} higher than Case 2.

On the other hand, if the goal is to achieve cooling temperature substantially below ambient temperature, Case 2 is better. For Case 2, the absorption from the ambient is low as the atmosphere is transparent, while, for Case 1, absorption from the ambient is significant due to absorption of the cooler in wavelengths outside the transparency window.[25] Achieving such low temperatures requires high vacuum to minimize parasitic conduction and convection.[21] If such parasitic mechanisms are present, expanding the bandwidth of thermal emission is likely to be beneficial despite the increase in sky radiation absorption as shown in Figure 4b.

The above discussion shows why the polymer-silica-mirror achieves such good performance despite absorbing atmospheric radiation. Due to convection and conduction, the steady-state temperature only minimally differs from that of the atmosphere, thus decreasing the influence of the atmospheric radiation and making the near-unity emissivity over a broad bandwidth beneficial. The result is a net cooling power density of 127 Wm^{-2} at ambient temperature of 300 K under AM 1.5 solar irradiation, 20 Wm^{-2} higher than the silica-mirror and more than twice of that achieved by the nanophotonic structure.[6] The predicted steady-state temperature at zero net cooling power using the measured $h_{con} = 10$ $Wm^{-2}K^{-1}$ is 8.7

°C below ambient under direct sunlight, in good agreement with our measurement.

In summary, we have shown that abundant materials with strong infrared emission over a broad bandwidth such as fused silica and PDMS are capable of radiative cooling with performance exceeding that of more complex nanophotonic structures. For applications in which the desired temperature is not substantially different from ambient temperature, a radiative cooler with near unity emissivity over a broad infrared spectrum will achieve better performance than one that emits only in the atmospheric window. The presented radiative cooler can be easily realized with common bulk materials such as fused silica wafers with a metallic back reflector. Further improvements in the present cooler can be achieved if structure can be designed to reduce sunlight absorption in the ultraviolet. Our work advances the application of passive radiative cooling for applications such as dry cooling of power plants.

Acknowledgement

This work is part of the 'Light-Material Interactions in Energy Conversion' Energy Frontier Research Center funded by the US Department of Energy, Office of Science, Office of Basic Energy Sciences under Award Number DE-SC0001293. The authors thank Prof. George Rossman for FTIR assistance, the Kavli Nanoscience Institute at Caltech for cleanroom facilities, and the Molecular Materials Research Center of the Beckman Institute at Caltech for UV/vis/NIR measurement.

References

(1) Liu, X.; Tyler, T.; Starr, T.; Starr, A. F.; Jokerst, N. M.; Padilla, W. J. Taming the blackbody with infrared metamaterials as selective thermal emitters. *Phys. Rev. Lett.* **2011**, *107*, 045901.

(2) Greffet, J.-J.; Carminati, R.; Joulain, K.; Mulet, J.-P.; Mainguy, S.; Chen, Y. Coherent emission of light by thermal sources. *Nature* **2002**, *416*, 61–64.

(3) Schuller, J. A.; Taubner, T.; Brongersma, M. L. Optical antenna thermal emitters. *Nat. Photon.* **2009**, *3*, 658–661.

(4) De Zoysa, M.; Asano, T.; Mochizuki, K.; Oskooi, A.; Inoue, T.; Noda, S. Conversion of broadband to narrowband thermal emission through energy recycling. *Nat. Photon.* **2012**, *6*, 535–539.

(5) Yeng, Y. X.; Ghebrebrhan, M.; Bermel, P.; Chan, W. R.; Joannopoulos, J. D.; Soljačić, M.; Celanovic, I. Enabling high-temperature nanophotonics for energy applications. *Proc. Natl. Acad. Sci.* **2012**, *109*, 2280–2285.

(6) Raman, A. P.; Anoma, M. A.; Zhu, L.; Rephaeli, E.; Fan, S. Passive radiative cooling below ambient air temperature under direct sunlight. *Nature* **2014**, *515*, 540–544.

(7) Inoue, T.; De Zoysa, M.; Asano, T.; Noda, S. Realization of dynamic thermal emission control. *Nat. Mater.* **2014**, *13*, 928–931.

(8) Zhu, L.; Raman, A. P.; Fan, S. Radiative cooling of solar absorbers using a visibly transparent photonic crystal thermal blackbody. *Proc. Natl. Acad. Sci.* **2015**, *112*, 12282–12287.

(9) Bierman, D. M.; Lenert, A.; Chan, W. R.; Bhatia, B.; Celanović, I.; Soljačić, M.; Wang, E. N. Enhanced photovoltaic energy conversion using thermally based spectral shaping. *Nat. Energy* **2016**, *1*, 16068.

(10) Ilic, O.; Bermel, P.; Chen, G.; Joannopoulos, J. D.; Celanovic, I.; Soljačić, M. Tailoring high-temperature radiation and the resurrection of the incandescent source. *Nat. Nanotechnol.* **2016**, *11*, 320–324.

(11) Zhou, L.; Tan, Y.; Wang, J.; Xu, W.; Yuan, Y.; Cai, W.; Zhu, S.; Zhu, J. 3D self-assembly of aluminium nanoparticles for plasmon-enhanced solar desalination. *Nat. Photon.* **2016**, *10*, 393–398.

(12) Rephaeli, E.; Raman, A.; Fan, S. Ultrabroadband photonic structures to achieve high-performance daytime radiative cooling. *Nano Lett.* **2013**, *13*, 1457–1461.

(13) Granqvist, C.; Hjortsberg, A. Surfaces for radiative cooling: Silicon monoxide films on aluminum. *Appl. Phys. Lett.* **1980**, *36*, 139–141.

(14) Gentle, A.; Aguilar, J.; Smith, G. Optimized cool roofs: Integrating albedo and thermal emittance with R-value. *Sol. Energ. Mat. Sol. Cells* **2011**, *95*, 3207–3215.

(15) Shi, N. N.; Tsai, C.-C.; Camino, F.; Bernard, G. D.; Yu, N.; Wehner, R. Keeping cool: Enhanced optical reflection and radiative heat dissipation in Saharan silver ants. *Science* **2015**, *349*, 298–301.

(16) Hsu, P.-C.; Song, A. Y.; Catrysse, P. B.; Liu, C.; Peng, Y.; Xie, J.; Fan, S.; Cui, Y. Radiative human body cooling by nanoporous polyethylene textile. *Science* **2016**, *353*, 1019–1023.

(17) Michell, D.; Biggs, K. Radiation cooling of buildings at night. *Appl. Energy* **1979**, *5*, 263–275.

(18) Nilsson, T. M.; Niklasson, G. A. Radiative cooling during the day: simulations and experiments on pigmented polyethylene cover foils. *Sol. Energ. Mat. Sol. Cells* **1995**, *37*, 93–118.

(19) Nilsson, T. M.; Niklasson, G. A.; Granqvist, C. G. A solar reflecting material for radiative cooling applications: ZnS pigmented polyethylene. *Sol. Energ. Mat. Sol. Cells* **1992**, *28*, 175–193.

(20) Catalanotti, S.; Cuomo, V.; Piro, G.; Ruggi, D.; Silvestrini, V.; Troise, G. The radiative cooling of selective surfaces. *Sol. Energy* **1975**, *17*, 83–89.

(21) Chen, Z.; Zhu, L.; Raman, A.; Fan, S. Radiative cooling to deep sub-freezing temperatures through a 24-h day–night cycle. *Nat. Commun.* **2016**, *7*, 13729.

(22) Zhu, L.; Raman, A.; Fan, S. Color-preserving daytime radiative cooling. *Appl. Phys. Lett.* **2013**, *103*, 223902.

(23) Gentle, A. R.; Smith, G. B. Radiative heat pumping from the earth using surface phonon resonant nanoparticles. *Nano Lett.* **2010**, *10*, 373–379.

(24) Hossain, M. M.; Jia, B.; Gu, M. A metamaterial emitter for highly efficient radiative cooling. *Adv. Opt. Mater.* **2015**, *3*, 1047–1051.

(25) Huang, Z.; Ruan, X. Nanoparticle embedded double-layer coating for daytime radiative cooling. *Int. J. Heat Mass Transfer* **2017**, *104*, 890–896.

(26) IR Transmission Spectra, Gemini Observatory Kernel Description. `http://www.gemini.edu/?q=node/10789`, accessed Nov. 20, 2016.

Table of Contents Graphic